Synthesis and Optical, Electrochemical, and Electron-Transporting Properties of Silicon-Bridged Bithiophenes

Joji Ohshita,*,† Mitsunori Nodono,† Hiroyuki Kai,† Tsuguo Watanabe,† Atsutaka Kunai,*,† Kenji Komaguchi,† Masaru Shiotani,† Akira Adachi,‡ Koichi Okita,‡ Yutaka Harima,§ Kazuo Yamashita,§ and Mitsuo Ishikawa||

Department of Applied Chemistry, Faculty of Engineering, Hiroshima University, Higashi-Hiroshima 739-8527, Japan, Japan Chemical Innovation Institute, Tsukuba Research Center (D-7), 2-1-6 Sengen, Tsukuba 305-0047, Japan, Division of Material and Life Sciences, Faculty of Integrated Arts and Sciences, Hiroshima University, Higashi-Hiroshima 739-8521, Japan, and Department of Chemical Technology, Kurashiki University of Science and the Arts, 2640 Nishinoura, Tsurashima, Kurashiki 712-8051, Japan

Received November 10, 1998

A series of bithiophene derivatives bearing an intramolecular monosilanylene or disilanylene bridge between the β,β'-positions were synthesized, and their properties were investigated. UV spectral and cyclic voltammetric analyses of the silicon-bridged bithiophenes indicated that they have lower lying LUMOs, relative to those for bithiophene and methylene bridged bithiophenes, probably due to $\sigma^*-\pi^*$ interaction between the silicon atom(s) and bithiophene π-orbitals, in good agreement with the results of theoretical calculations using simplified model compounds based on RHF/6-31G. The silicon-bridged bithiophenes exhibit high electron-transporting properties, and triple-layer-type electroluminescent (EL) devices, using the silicon-bridged bithiophenes, tris(8-quinolinolato)aluminum(III) complex (Alq), and *N*,*N*′-diphenyl-*N*,*N*′-di-*m*-tolylbiphenyl-4,4′-diamine (TPD) as the electron-transporting, emitting, and hole-transporting layers, respectively, emitted strong EL.

Introduction

π-Conjugated systems containing silole rings are of current interest because of their unique optical and electrical properties.[1−5] Both experimental and theoretical studies have demonstrated that the silole ring system possesses a particularly low-lying LUMO, presumably due to the orbital interaction between the σ^* orbital of the silole silicon atom and the π^*-orbital of the butadiene fragment, namely $\sigma^*-\pi^*$ conjugation.[2] The low-lying LUMO is the origin of the unique properties, including the small band gap and high electron affinity, which give rise to the potential utilities of the silole-containing conjugated systems as the novel functionality materials. Tamao et al. have reported the synthesis of several cooligomers composed of 2,5-silole and pyrrole units and demonstrated that they exhibit high electron-transporting properties, being applicable to electroluminescent (EL) devices.[3] It has been also demonstrated that highly extended conjugation takes place along the backbone in the alternating polymers of silole-2,5-diyl and oligo(2,5-thienylene) units, leading to small band gaps and highly conducting properties of the doped polymers.[4] In addition, the synthesis of polymers having 2,5-diethynylsilole units in the backbone with a small band gap has been recently reported.[5]

Oligothiophenes, on the other hand, have been actively studied as functionality materials, such as photo- and electroluminescent, conducting, and nonlinear optical materials.[6] In an effort to develop new conjugated systems based on $\sigma-\pi$ conjugation,[7] we have synthesized poly[disilanyleneoligo(2,5-thienylenes)] ($[SiR_2SiR_2(C_4H_2S)_m]_n$, $m = 1-5$) and found that orbital interaction between the Si−Si σ-bond and oligothiophene π-orbitals is operative, although the longer oligothienylene unit results in a lower degree of $\sigma-\pi$ conjugation.[8] Recently, we have synthesized dithienosiloles which have a bithiophene unit that bears an intramolecular silylene bridge between the β,β'-positions, forming a silole ring

† Faculty of Engineering, Hiroshima University.
‡ Japan Chemical Innovation Institute.
§ Faculty of Integrated Arts and Sciences, Hiroshima University.
|| Kurashiki University of Science and the Arts.

(1) (a) Tamao, K.; Yamaguchi, S.; Shiozaki, M.; Nakagawa, Y.; Ito, Y. *J. Am. Chem. Soc.* **1992**, *114*, 5867. (b) Tamao, K.; Yamaguchi, S.; Shiro, M. *J. Am. Chem. Soc.* **1994**, *116*, 11715. (c) Sanji, T.; Sakai, T.; Kabuto, C.; Sakurai, H. *J. Am. Chem. Soc.* **1998**, *120*, 4552. (d) Kanno, K.-I.; Ichinohe, M.; Kabuto, C.; Kira, M. *Chem. Lett.* **1998**, 99.

(2) (a) Yamaguchi, S.; Tamao, K. *Bull. Chem. Soc. Jpn.* **1996**, *69*, 2327. (b) Yamaguchi, S. *Synth. Met.* **1996**, *82*, 149. (c) Hong, S. Y.; Song, J. M. *Chem. Mater.* **1997**, *9*, 297.

(3) (a) Tamao, K.; Ohno, S.; Yamaguchi, S. *Chem. Commun.* **1996**, 1873. (b) Tamao, K.; Uchida, M.; Izumikawa, T.; Furukawa, K.; Yamaguchi, S. *J. Am. Chem. Soc.* **1996**, *116*, 11974.

(4) (a) Tamao, K.; Yamaguchi, S.; Shiozaki, M.; Nakagawa, Y.: Ito, Y. *J. Am. Chem. Soc.* **1992**, *114*, 5867. (b) Tamao, K.; Yamaguchi, S.; Ito, Y.; Matsuzaki, Y.; Yamabe, T.; Fukushima, M.; Mori, S. *Macromolecules* **1995**, *28*, 8668.

(5) (a) Yamaguchi, S.; Iimura, K.; Tamao, K. *Chem. Lett.* **1998**, 89. (b) Ohshita, J.; Mimura, H. Arase, N.; Nodono, M.; Kunai, A.; Komaguchi, K.; Shiotani, M.; Ishikawa, M. *Macromolecules* **1998**, *31*, 7985.

(6) For example, see: Hotta, S. In *Organic Conductive Molecules and Polymers*; Nalwa, H. S., Ed.; Wiley: New York, 1997; Vol. 2, Chapter 8.

(7) Ohshita, J.; Kunai, A. *Acta Polym.* **1998**, *49*, 379.

(8) (a) Kunai, A.; Ueda, T.; Horata, K.; Toyoda, E.; Ohshita, J.; Ishikawa, M.; Tanaka, K. *Organometallics* **1996**, *15*, 2000.

10.1021/om980918n CCC: $18.00
Publication on Web 03/19/1999

Scheme 1

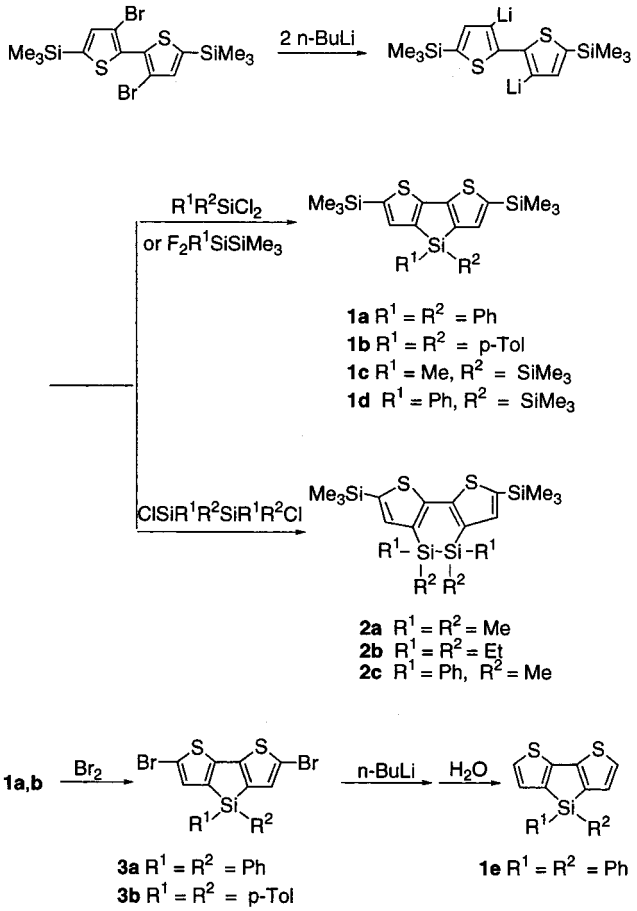

fused with two thiophene rings, in the hope that the silicon bridge might exert some positive influence on the electronic states of the bithiophene system to facilitate conjugation in the system.[9] First, the interaction between the silicon σ^*-orbital and bithiophene π^*-orbital would lower the LUMO level, as observed for simple siloles. Second, it is postulated that the existence of the silicon bridge forces the bithiophene unit to retain a syn configuration with high planarity to facilitate the overlap of the π-orbitals. Third, sufficient interaction should take place between the electron-deficient silole ring and electron-rich bithiophene system.

In this paper, we report the synthesis and optical and electrochemical properties of dithienosiloles in detail. In addition, we have prepared disilanylene-bridged bithiophenes, dithienodisilacyclohexadienes, and studied their properties in comparison with those of dithienosiloles, in order to discover how the structure of the silicon bridge affects the electronic state of the bithiophene derivatives. Results on molecular orbital calculations using simplified models and applications of the silicon-bridged bithiophenes to the electron-transporting materials for triple-layer electroluminescent devices are also described.

Results and Discussion

Synthesis of Dithienosiloles and Dithienodisilacyclohexadienes. The reactions of 3,3′-dilithio-5,5′-bis(trimethylsilyl)-2,2′-bithiophene, prepared by treating 3,3′-dibromo-5,5′-bis(trimethylsilyl)-2,2′-bithiophene with 2 equiv of *n*-butyllithium, with dichlorodiphenylsilane and dichlorodi-*p*-tolylsilane gave 4,4-diphenyl- and 4,4-di-*p*-tolyl-2,6-bis(trimethylsilyl)dithieno[3,2-*b*:2′,3′-*d*]-silole (**1a**,**b**) in 73% and 52% isolated yields, respectively, as shown in Scheme 1. Similarly, 2,4,6-tris-(trimethylsilyl)dithienosiloles (**1c**,**d**) were obtained in 43% and 20% yields from the reactions of dilithiobis-(trimethylsilyl)bithiophene with the respective 1,1-difluorodisilanes. In these reactions, using difluorodisilanes instead of 1,1-dichlorodisilanes was required to obtain the dithienosiloles in high yields. In fact, a similar reaction with 1,1-dichlorotetramethyldisilane gave a trace of **1c** and a nearly quantitative yield of 5,5′-bis(trimethylsilyl)bithiophene, after hydrolysis of the reaction mixture. This may be ascribed to the steric protection of the dichlorosilyl unit by a trimethylsilyl group in the dichlorodisilane. In contrast to 1,1-dichlorodisilanes, 1,2-dichlorodisilanes reacted readily with dilithiobis(trimethylsilyl)bithiophene to afford 2,7-bis-(trimethylsilyl)dithieno[3,2-*c*:2′,3′-*e*]disilacyclohexadienes (**2a**−**c**) in 33%, 29%, and 37% yields, respectively. Compound **2c** was obtained as a 30:70 mixture of cis and trans isomers, and the trans isomer was isolated readily from the mixture as a solid by recrystallization.

The trimethylsilyl groups at the 2,6-positions in the dithienosiloles were readily replaced with bromine atoms. Thus, treatment of **1a**,**b** with 2 equiv of bromine afforded 2,6-dibromodithienosiloles **3a**,**b** in 66% and 65% yields, respectively. In these reactions, only Me_3-Si−C bond cleavage occurred and no products arising from cleavage of the ring Si−C bonds were obtained. Dilithiation of **3a** with 2 equiv of *n*-butyllithium in ether, followed by hydrolysis of the resulting dilithiodithienosilole, gave compound **1e** in 77% yield.

Table 1. Properties of Dithienosiloles and Dithienodisilacyclohexadienes

compd	λ_{max}/nm (ϵ) absorpn[a]	λ_{max}/nm (ϵ) emissn[a]	first oxidn potential[b]/V vs SCE
1a	356 (10 220)	425	1.22
1b	358 (15 020)	420	1.25
1c	350 (17 320)	419	1.08
1d	352 (29 790)	419	1.08
1e	356 (6 080)	420	1.16
2a	350 (23 070)	419	1.05
2b	352 (15 360)	432	1.15
trans-**2c**	353 (18 190)	424	1.15

[a] In THF. [b] Peak potential measured on a 4 mM solution in acetonitrile containing 100 mM of Et_4NBF_4 using GC and Pt plate as working and counter electrodes at a scan rate of 20 mV/s.

Optical and Electrochemical Properties of Dithienosiloles and Dithienodisilacyclohexadienes. Table 1 summarizes optical and electrochemical properties of the dithienosiloles and dithienodisilacyclohexadienes. The absorption and emission bands in THF appear around 350 and 420 nm, regardless of the nature of the substituents on the silicon atom(s), although a slight blue shift (3−8 nm) is observed for compounds **1c**,**d** and **2a**-**c** having an Si−Si bond from **1a**,**b**,**e**. The absorption and emission maxima are at shorter energy by about 70 and 130 nm, respectively, than those of 2,5-dithienylsilole derivatives reported by Tamao et al.,[1a,3b] but the absorptions are at longer wavelength than those of 2,5-dibromo-1,1-diethyl-3,4-diphenylsilole (λ_{max} = 326

(9) (a) Ohshita, J.; Nodono, M.; Watanabe, T.; Ueno, Y.; Kunai, A.; Harima, Y.; Yamashita, K.; Ishikawa, M. *J. Organomet. Chem.* **1998**, *553*, 487. (b) Adachi, A.; Ohshita, J.; Kunai, A.; Kido, J.; Okita, K. *Chem. Lett.*, in press. For related works see ref 10.

Chart 1

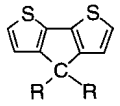

4a R = H
4b R = alkyl

nm),[1b] 2,2′-bithiophene (λ_{max} = 304 nm), and methylene-bridged bithiophene **4a** (Chart 1; λ_{max} = 323 nm).[11] The remarkable red shifts of the absorption maxima of dithienosiloles and disilacyclohexadienes from bithiophene and **4a** clearly indicate that introduction of a silicon bridge between two thiophene rings favors conjugation in the tricyclic system, as stated in the Introduction. Band gaps estimated from the onsets of the UV absorptions are in the range 3.2−3.3 eV for these silicon-bridged bithiophenes, which are again little affected by the nature of the substituents and the length of the silicon bridge.

There is no significant dependence of the absorption maxima on the solvent polarity, and changing the solvent from THF to cyclohexane resulted in a slight blue shift by only 0−2 nm, indicating that CT-type interaction in these compounds is weak if at all present. Emission maxima also shift, depending on the solvent polarity, by 0−6 nm, but without a definite direction.

The cyclic voltammograms (CVs) of dithienosiloles and dithienodisilacyclohexadienes were measured in acetonitrile. The CV curve of compound **1a** on the first scan is depicted in Figure 1 as a typical example, which reveals an irreversible anodic peak. The peak current is directly proportional to the substrate concentration and shows square-root dependence as the function of the sweep rate, being characteristic of diffusion-controlled processes. Repetitive cycling of the potential between 0 and 1.2 V vs SCE led to the development of a new oxidation peak and its reductive couple at 0.84 and 0.46 V vs SCE, respectively, with the growing of a dark red conducting polymer film on the anode. The conductivity of the resulting film was determined to be 2×10^{-6} S/cm in a doped state, although we have not yet obtained any evidence to characterize the polymer structure.[12]

The other dithienosiloles and dithienodisilacyclohexadienes also exhibit irreversible CVs with an oxidation peak appearing at 1.05−1.25 V vs SCE, as listed in Table 1, accompanied by the formation of dark red solids on the anode on multiple scans. Although we could determine no real $E_{1/2}$ values because of the absence of the reductive counterpart in the CVs, the structural similarity of these compounds and the diffusion-controlled process for the oxidation step would permit us to estimate a relative order of HOMO levels for the compounds by comparing the oxidation peak potentials. Despite the irreversibility of the peaks, a series of compounds with similar structures would involve the same degree of solvation and undergo similar reaction from the cation species, implying that potential shifts due to these factors would compensate each other.

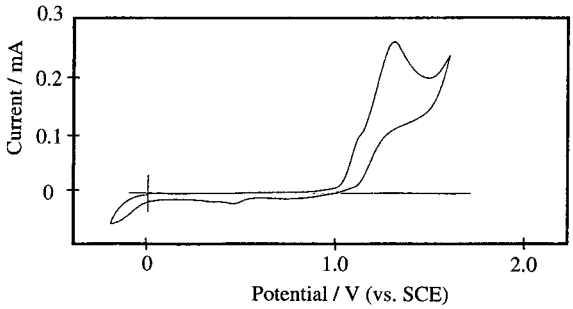

Figure 1. CV profile of compound **1a** in acetonitrile on the first scan.

The oxidation potentials are essentially the same but slightly higher as compared with those reported for several dialkylmethylene-bridged bithiophenes **4b** (0.99 V vs SCE).[13] The peak potentials of dithienosiloles **1a**,**b**, having no Si−Si bonds, are higher by 0.1−0.2 V than those of trimethylsilyl-substituted dithienosiloles **1c**,**d** and disilacyclohexadienes **2a**−**c** with the same trimethylsilyl substituents on the thiophene rings. Assuming that oxidation peak potentials obtained by CV measurements relate to HOMO levels of the compounds, the relative HOMO energy levels may be slightly elevated in the orders **1a**,**b** < **1c**,**d** and **2a**−**c** < **4**.

Crystal Structures of 2a,c. The crystal structures of compounds **2a** and *trans*-**2c** were determined by X-ray single-crystal diffraction studies. ORTEP drawings of them are depicted in Figures 2 and 3. Cell dimensions, data collection and refinement parameters, and selected bond distances and angles are given in Tables 2−4. As can be seen in Figures 2 and 3, compounds **2a**,**c** have essentially identical dithienodisilacyclohexadiene units which involve a twisted bithiophene system with a twisting angle of 20.2° for **2a** and 24.6° for *trans*-**2c** between two thiophene rings. This is in contrast to the crystal structure of compound **1e**, whose X-ray study indicates complete planarity in the tricyclic system,[9] although the rather small twisting angles for **2a**,**c** still indicate high planarity in these compounds.

The thiophene rings are almost planar, with maximum deviations from the mean plane of the thiophene ring of 0.008 Å for C8 in **2a** and 0.02 Å for C3 and C5−8 in **2c**. Sums of bond angles at sp^2 carbons in disilacyclohexadiene rings range from 359.8 to 360°. These are indicative of the absence of evident ring strain in these compounds. There are no intermolecular contacts in the packing structures of **2a**,**c**.

Theoretical Calculations on Model Compounds. To learn more about the electronic structures of silicon-bridged bithiophenes, we carried out theoretical calculations on simplified model compounds **1f**, **2d**, **4a**, and **5** based on RHF/6-31G. The relative energy levels for the model compounds are depicted in Figure 4. As can be seen in Figure 4, the band gaps of **1f** and **2d** were calculated to be much smaller relative to those of **4a** and **5**. The differences in LUMO energy levels for silicon-bridged bithiophenes **1f** and **2d** and the carbon-

(10) Chen, W.; Ijadi-Maghsooddi, S.; Barton, T. J. *Polym. Prepr.* **1997**, *38*, 189.
(11) Kraak, A.; Wiersema, A. K.; Jordens; P.; Wynberg, H. *Tetrahedron* **1968**, *24*, 3381.
(12) Anodic polymerization of α-silated thiophenes leading to polythiophenes has been reported: Sauvajol, J. L.; Lère-Porte, J. P.; Moreau, J. J. E. In *Organic Conductive Molecules and Polymers*; Nalwa, H. S., Ed.; Wiley: New York, 1997; Vol. 2, Chapter 14.
(13) Zotti, G.; Schiavon, G.; Berlin, A.; Fontana, G.; Pagani, G. *Macromolecules* **1994**, *27*, 1938.

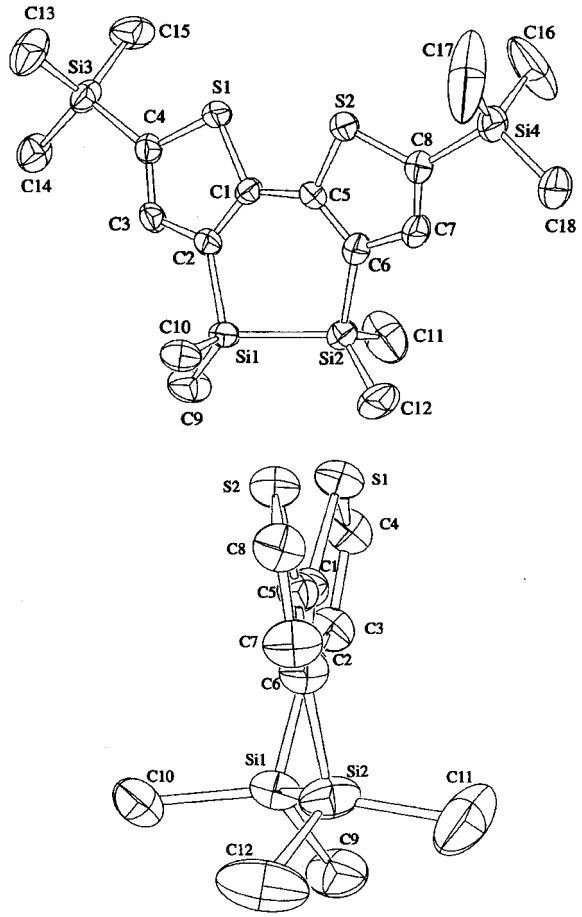

Figure 2. ORTEP drawing of compound **2a**: (a, top) top view; (b, bottom) side view. Protons are omitted for clarity. For the side view, trimethylsilyl groups are also omitted.

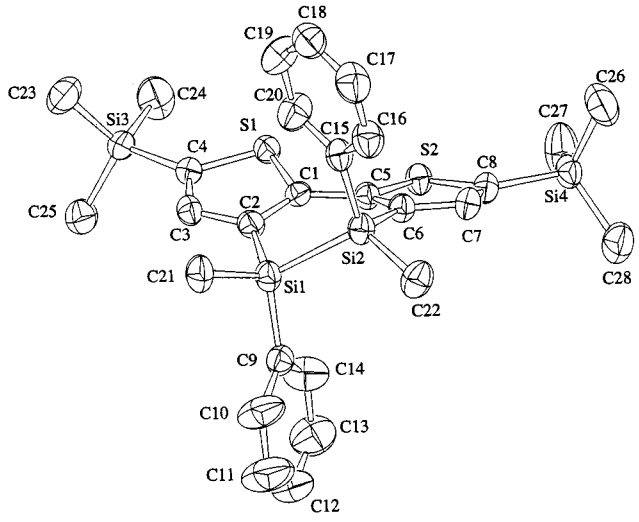

Figure 3. ORTEP drawing of *trans*-**2c**.

bridged analogue **4a** are calculated to be much larger (0.59−0.69 eV) than those of HOMO levels (0.27−0.43 eV), being responsible for the smaller HOMO−LUMO gaps for **1f** and **2d** relative to that for **4a**. These results are in agreement with the experimental observations, i.e., red-shifted UV absorption maxima and similar oxidation peak potentials for silicon-bridged bithiophenes relative to the carbon-bridged analogues.

Tamao et al. have previously reported similar results of MO calculations for some heterocycles, including silole, pyrrole, furan, and thiophene; of these silole has the smallest HOMO−LUMO gap, arising primarily from its lower-lying LUMO.[2a]

Table 2. Crystal Data, Experimental Conditions, and Summary of Structural Refinement for 2a and *trans*-2c

	2a	*trans*-**2c**
mol formula	$C_{18}H_{32}S_2Si_4$	$C_{28}H_{36}S_2Si_4$
mol wt	424.91	549.05
space group	*Cc*	*C*2/*c*
cell dimens		
a, Å	20.418(4)	39.001(5)
b, Å	11.335(2)	8.698(5)
c, Å	11.062(2)	18.580(4)
β, deg	93.06(2)	98.20(1)
V, Å^3	2556.9(9)	6238(3)
Z	4	8
D_{calcd}, Mg/m^3	1.104	1.169
F_{000}	912.00	2336.00
cryst size, mm^3	0.5 × 0.5 × 0.4	0.4 × 0.2 × 0.1
cryst color	light yellow	colorless
μ, mm^{-1}	3.670	2.1026
diffractometer	Rigaku AFC-6S	Rigaku AFC-6S
temp, K	233	233
wavelength, Å	1.5418 (Cu Kα)	1.5418 (Cu Kα)
monochromator	graphite cryst	graphite cryst
scan type	$\omega-2\theta$	$\omega-2\theta$
scan speed, deg/min	4	4
scan width, deg	$0 < 2\theta < 125.9$	$0 < 2\theta < 126.1$
diffraction geom	symmetrical A	symmetrical A
no. of unique rflns	2041	4927
no. of obsd rflns ($I > 3\sigma(I)$)	1791	3229
R	0.042	0.038
R_w[a]	0.055	0.043

[a] Weighting scheme is $(\sigma(F_o)^2 + 0.0004|F_o|^2)^{-1}$.

Table 3. Selected Distances (Å) and Angles (deg) for Compound 2a with Their Esd's in Parentheses

Si1−Si2	2.320(3)	Si1−C2	1.878(8)	Si2−C6	1.872(9)
S1−C1	1.738(7)	S1−C4	1.722(8)	S2−C5	1.741(8)
S2−C8	1.733(8)	C1−C2	1.38(1)	C1−C5	1.45(1)
C2−C3	1.42(1)	C3−C4	1.39(1)	C5−C6	1.37(1)
C6−C7	1.43(1)	C7−C8	1.35(1)		

Si2−Si1−C2	100.5(3)	Si1−Si2−C6	101.6(3)
C1−S1−C4	93.6(4)	C5−S2−C8	92.5(4)
S1−C1−C2	110.3(6)	S1−C1−C5	120.4(6)
C2−C1−C5	129.1(7)	Si1−C2−C1	123.4(6)
Si1−C2−C3	124.4(6)	C1−C2−C3	112.1(7)
C2−C3−C4	114.8(7)	S1−C4−C3	109.1(6)
S2−C5−C1	120.1(6)	S2−C5−C6	110.9(6)
C1−C5−C6	129.1(7)	Si2−C6−C5	124.4(6)
Si2−C6−C7	124.1(6)	C5−C6−C7	111.5(8)
C6−C7−C8	115.3(8)	S2−C8−C7	109.7(6)

Table 4. Selected Distances (Å) and Angles (deg) for Compound *trans*-2c with Their Esd's in Parentheses

Si1−Si2	2.338(2)	Si1−C2	1.878(4)	Si2−C6	1.877(4)
S1−C1	1.725(4)	S1−C4	1.723(4)	S2−C5	1.736(4)
S2−C8	1.724(4)	C1−C2	1.381(5)	C1−C5	1.455(5)
C2−C3	1.421(6)	C3−C4	1.369(6)	C5−C6	1.379(5)
C6−C7	1.412(5)	C7−C8	1.366(5)		

Si2−Si1−C2	103.3(1)	Si1−Si2−C6	100.4(1)
C1−S1−C4	93.4(2)	C5−S2−C8	93.1(2)
S1−C1−C2	111.0(3)	S1−C1−C5	120.1(3)
C2−C1−C5	128.8(4)	Si1−C2−C1	122.6(3)
Si1−C2−C3	126.5(3)	C1−C2−C3	110.9(3)
C2−C3−C4	115.8(4)	S1−C4−C3	108.8(3)
S2−C5−C1	119.7(3)	S2−C5−C6	110.6(3)
C1−C5−C6	129.7(3)	Si2−C6−C5	122.3(3)
Si2−C6−C7	126.3(3)	C5−C6−C7	111.4(3)
C6−C7−C8	115.9(4)	S2−C8−C7	109.0(3)

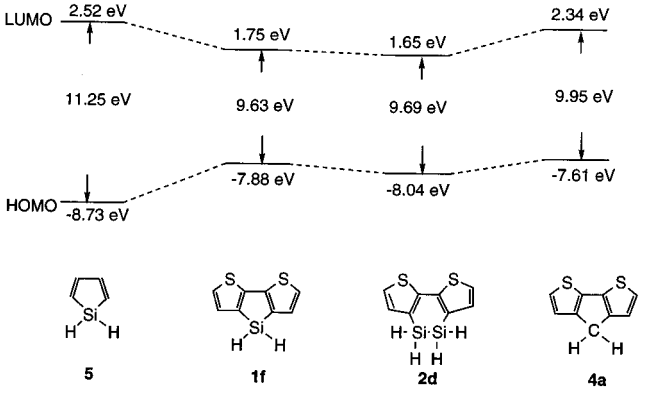

Figure 4. Relative energy levels of HOMO and LUMO of compounds **1f**, **2d**, **4a**, and **5** derived from MO calculations at the RHF/6-31G level.

Although the electronic states of the actual compounds derived from UV and CV measurements can be approximately reproduced by the theoretical calculations on the model compounds, there is slight but certain disagreement. Thus, the HOMO level of **1f** was predicted to be a little higher than that of **2d**, in contrast to the results of CV measurements, which suggest slightly lower HOMO levels for diaryldithienosiloles **1a**,**b** than those for not only silyl-substituted dithienosiloles **1c**,**d** but also disilacyclohexadienes **2a**−**c**. It is not likely that the presence of two aryl groups in **1a** and **1b** is responsible for their higher oxidation peak potentials. Replacement of methyl substituents on the silicon bridge of compound **2a** with ethyl groups leads to a 0.1 V higher shift of the peak of **2b**, while the influence of phenyl groups is almost the same as observed for **2c**. Furthermore, there can be seen no evident influence of the introduction of a phenyl group into the dithienosilole silicon atom, as indicated by the same oxidation potentials for **1c** and **1d**.

The slight deviation from planarity as indicated by the X-ray diffraction studies on compounds **2a** and *trans*-**2c** would be, therefore, a reason for the disagreement between the results of CV analyses and theoretical predictions which were carried out on planar model compound **2d**.

EL Properties of Silicon-Bridged Bithiophenes. To evaluate the EL properties of silicon-bridged bithiophenes, we fabricated multilayer devices (type I) having a silicon-bridged bithiophene layer as the electron transport by vacuum deposition. For comparison, a typical two-layer device without the silicon-bridged bithiophene layer was also fabricated as type II. The device structure and the thickness of each layer are ITO/TPD (40 nm)/Alq (50 nm)/silicon-bridged bithiophene (10−20 nm)/Mg:Ag for type I and ITO/TPD (40 nm)/Alq (60 nm)/Mg:Ag for type II.

We examined compounds **1a**,**b**,**e** and *trans*-**2c**, which have sufficiently high melting points, as the electron-transporting substances for type I EL devices. Figure 5 illustrates the current density−voltage (I−V) characteristics of the type I devices with compounds **1b** and *trans*-**2c** and a type II device. The current density of the type I device with **1b** is always higher than that of type II at any operating voltage in the measurement range 4−14 V. The I−V plots of the type I device with **1e** are in the middle of those of the type I device with

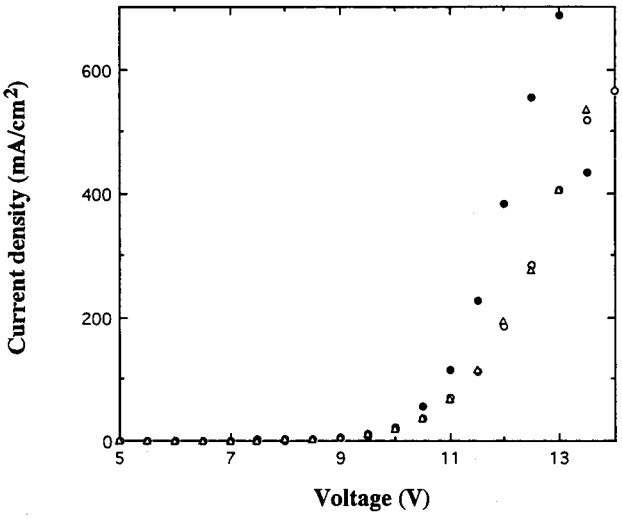

Figure 5. Plots of operating voltage vs current density for a type I device with (●) compound **1b** and (△) *trans*-**2c** and (○) a type II device.

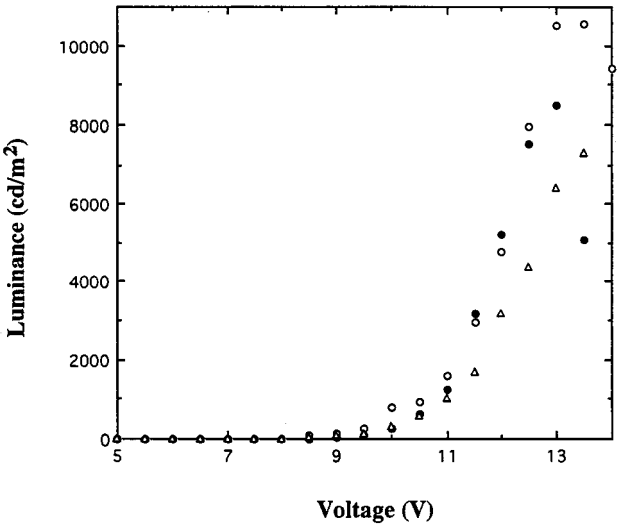

Figure 6. Plots of operating voltage vs luminescence for a type I device with (●) compound **1b** and (△) *trans*-**2c** and (○) a type II device.

1b and type II device in the same measurement range, while the devices with **1a** and *trans*-**2c** always exhibit a slightly lower current density than the type II device. These results indicate that silicon-bridged bithiophene layers have comparable or even higher electron-transporting properties relative to the layer of Alq, which is known as a typical and efficient electron-transporting substance, and are consistent with the low-lying LUMO levels of silicon-bridged bithiophenes calculated from ionization potentials and electronic absorption spectra which are comparable to that of Alq (3.1 eV).

From both types of the devices, green electroluminescence was observed and the EL spectra were identical with the photoluminescence (PL) spectrum of a vacuum-deposited film of Alq, implying that the EL originated from the emission of the Alq layer. As shown in Figure 6, the luminance of the devices increased as the operating voltage was increased and reached the maximum values of ca. 8000 cd/m^2 at 13 V of the operating voltage for the type I device with **1b**. Applying higher voltage for the devices, however, resulted in a rapid decrease

of current density and luminescence, probably due to the decomposition of the silicon-bridged bithiophene layer in the devices by melting or crystallization. The intensity of the luminescence up to 13 V obtained from a type I device with **1b** was nearly the same as that from a type II device, despite the higher current density of the type I device with **1b**. This is probably due to poor hole-blocking properties of dithienosiloles.

The origin of the dependence of I−V characteristics on the electron-transporting substance in type I devices is still unclear. However, it seems likely that factors other than just the LUMO energy levels of the silicon-bridged bithiophenes, including packing structures in the vapor-deposited layer, are important. Further study on the carrier injection mechanism of silicon-bridged bithiophenes has been undertaken, and the results will be published elsewhere.

Experimental Section

General Considerations. All reactions were carried out under an atmosphere of dry nitrogen. The usual workup mentioned in the following involves separating the organic layer, extracting the aqueous layer, drying the combined organic layer and the extracts, and evaporating the solvents, in that order. NMR spectra were recorded on JEOL Model JNM-EX 270 and JEOL Model JNM-LA 400 spectrometers. Mass spectra were measured with a Hitachi M80B spectrometer. UV spectra were measured on a Hitachi U-3210 spectrophotometer, and emission spectra were obtained by a Shimadzu RF5000 spectrophotometer. IR spectra were measured on a Perkin-Elmer FTIR Model 1600 spectrometer.

Materials. THF and ether were dried over sodium−potassium alloy and distilled just before use. Acetonitrile was distilled from P_2O_5 and stored in the dark under an argon atmosphere at 4 °C before use. The starting 3,3′,5,5′-tetrabromobithiophene was prepared as reported in the literature.[14]

Synthesis of 3,3′-Dibromo-5,5′-bis(trimethylsilyl)-2,2′-bithiophene. In a 1 L three-necked flask fitted with a dropping funnel were placed 20.1 g (41.8 mmol) of 3,3′,5,5′-tetrabromobithiophene and 500 mL of ether. To this was added 50.0 mL (83.6 mmol) of a 1.7 M *n*-butyllithium/hexane solution at −80 °C. The resulting mixture was warmed to 0 °C. After the resulting mixture was stirred at 0 °C for 6 h, 11.0 mL (83.6 mmol) of chlorotrimethylsilane was added to the mixture. The mixture was then hydrolyzed with water. After the usual workup, the resulting mixture was chromatographed on a silica gel column with hexane as eluent to give crude yellow solids, which were recrystallized from ethanol, affording 13.8 g (72% yield) of the title compound as pale yellow solids: mp 87−88 °C; MS *m*/*z* 466 (M^+); ^{1}H NMR (δ in $CDCl_3$) 0.35 (s, 18H, $SiMe_3$), 7.16 (s, 2H, thiophene ring protons); ^{13}C NMR (δ in $CDCl_3$) −0.39 ($SiMe_3$), 112.9 (C−Br), 133.9 (*C*-$SiMe_3$), 136.9 (C4 and C4′), 142.9 (C2 and C2′). Anal. Calcd for $C_{14}H_{20}Br_2S_2Si_2$: C, 35.90; H, 4.30. Found: C, 36.02; H, 4.31.

Synthesis of Dithienosilole 1a. In a 300 mL three-necked flask fitted with a dropping funnel were placed 6.09 g (13.0 mmol) of 3,3′-dibromo-5,5′-bis(trimethylsilyl)-2,2′-bithiophene and 180 mL of ether. To this was added 19.0 mL (31.2 mmol) of a 1.7 M *n*-butyllithium/hexane solution at −80 °C. After the resulting mixture was stirred at this temperature for 2 h, 3.0 mL (14.4 mmol) of dichlorodiphenylsilane was added to the mixture. The mixture was then warmed to room temperature and hydrolyzed with water. After the usual workup, the resulting mixture was chromatographed on a silica gel column with hexane as eluent to give crude dark yellow solids, which were recrystallized from ethanol, affording 4.62 g (73% yield) of **1a** as light yellow crystals: mp 158−160 °C; MS *m*/*z* 490 (M^+); ^{1}H NMR (δ in $CDCl_3$) 0.33 (s, 18H, Me_3Si), 7.24 (s, 2H, thiophene ring protons), 7.28−7.42 (m, 6H, Ph), 7.64 (dd, 4H, J = 8.1, 1.5 Hz, *o*-Ph protons); ^{13}C NMR (δ in $CDCl_3$) 0.1 ($SiMe_3$), 128.1, 130.2, 132.3, 135.5 (Ph), 136.5 (C3 and C5), 141.7 (C2 and C6), 142.2 (C7a and C7b), 155.6 (C3a and C4a). Anal. Calcd for $C_{26}H_{30}S_2Si_3$: C, 63.62; H, 6.16. Found: C, 63.43; H, 6.08.

Compounds **1b**−**d** and **2a**−**c** were prepared as described for **1a**, by using $(p\text{-tol})_2SiCl_2$, $Me_3SiSiMeF_2$, $Me_3SiSiPhF_2$, $(Me_2ClSi)_2$, $(Et_2ClSi)_2$, or $(PhMeClSi)_2$ instead of Ph_2SiCl_2.

Data for **1b**: 52% yield; light yellow solids; mp 133−135 °C; MS *m*/*z* 518 (M^+); ^{1}H NMR (δ in $CDCl_3$) 0.39 (s, 18H, $SiMe_3$), 2.38 (s, 6H, *p*-Me), 7.18 (s, 2H, thiophene ring protons), 7.23 (d, 4H, J = 7.8 Hz, tolyl ring protons), 7.54 (d, 4H, J = 7.8 Hz, tolyl ring protons); ^{13}C NMR (δ in $CDCl_3$) 0.1 ($SiMe_3$), 21.7 (*p*-Me), 128.6, 128.9, 135.6 (Tol), 136.9 (C3 and C5), 140.2 (Tol), 141.9 (C2 and C6), 142.2 (C7a and C7b), 155.4 (C3a and C4a); ^{29}Si NMR (δ in $CDCl_3$) −22.2 (silole Si), −6.9 (C−$SiMe_3$). Anal. Calcd for $C_{28}H_{34}S_2Si_3$: C, 64.81; H, 6.60. Found: C, 64.73; H, 6.65.

Data for **1c**: 43% yield; white solids; mp 58−59 °C; MS *m*/*z* 424 (M^+); ^{1}H NMR (δ in $CDCl_3$) 0.46 (s, 3H, Me−Si), 0.08 (s, 9H, Si−$SiMe_3$), 0.35 (s, 18H, C−$SiMe_3$), 7.16 (s, 2H, thiophene ring protons); ^{13}C NMR (δ in $CDCl_3$) −6.09 (Me−Si), −2.03 (Si−$SiMe_3$), 0.14 (C−Si*Me*$_3$), 136.2 (C3 and C5), 141.0 (C2 and C6), 145.1 (C7a and C7b), 153.6 (C3a and C4a); ^{29}Si NMR (δ in $CDCl_3$) −28.2 (silole Si), −17.5 (Me_3Si−Si), −7.05 (C−$SiMe_3$). Anal. Calcd for $C_{18}H_{32}S_2Si_4$: C, 50.87; H, 7.59. Found: C, 50.80; H, 7.60.

Data for **1d**: 20% yield; white solids: mp 97−98 °C; MS *m*/*z* 486 (M^+); ^{1}H NMR (δ in $CDCl_3$) 0.12 (s, 9H, Si−$SiMe_3$), 0.34 (s, 18H, C−$SiMe_3$), 7.24 (s, 2H, thiophene ring protons), 7.32−7.35 (m, 3H, Ph), 7.56−7.60 (m, 2H, *o*-Ph); ^{13}C NMR (δ in $CDCl_3$) −1.71 (Si−$SiMe_3$), 0.16 (C−Si*Me*$_3$), 128.1, 134.9, 129.3 (Ph), 133.3 (Ph *ipso*-C), 136.3 (C3 and C5), 141.5 (C2 and C6), 143.1 (C7a and C7b), 154.0 (C3a and C4a); ^{29}Si NMR (δ in $CDCl_3$) −30.6 (silole Si), −16.9 (Me_3Si−Si), −7.0 (C−$SiMe_3$); exact MS calcd for $C_{23}H_{34}S_2Si_4$ 486.1179, found 486.1178.

Data for **2a**: 33% yield; light yellow solids: mp 85−86 °C; MS *m*/*z* 424 (M^+); ^{1}H NMR (δ in $CDCl_3$) 0.33 (s, 12H, Me−Si), 0.34 (s, 18H, $SiMe_3$), 7.20 (s, 2H, thiophene ring protons); ^{13}C NMR (δ in $CDCl_3$) −3.1 (Me_2Si), 0.0 ($SiMe_3$), 135.1 (C3 and C6), 138.7, 139.8 (C2, C7, C8a, and C8b), 150.6 (C3a and C5a); ^{29}Si NMR (δ in $CDCl_3$) −34.0 ($SiMe_2$), −7.5 ($SiMe_3$). Anal. Calcd for $C_{18}H_{32}S_2Si_4$: C, 50.87; H, 7.59. Found: C, 50.85; H, 7.39.

Data for **2b**: 29% yield; light yellow liquid; MS *m*/*z* 480 (M^+); ^{1}H NMR (δ in $CDCl_3$) 0.32 (br s, 12H,C−CH_3), 0.84−1.03 (m, 8H, CH_2), 7.13 (s, 2H, thiophene ring protons); ^{13}C NMR (δ in $CDCl_3$) 0.0 ($SiMe_3$), 4.4 (CH_3), 8.5 (CH_2), 133.4 (C3 and C6), 138.2, 140.1 (C2, C7, C8a, and C8b), 151.3 (C3a and C5a); ^{29}Si NMR (δ in $CDCl_3$) −26.3 ($SiEt_2$), −8.4 ($SiMe_3$). Anal. Calcd for $C_{22}H_{40}S_2Si_4$: C, 54.93; H, 8.38. Found: C, 54.77; H, 8.62.

Compound **2c** was obtained as a mixture of cis and trans isomers in 37% yield. Recrystallization of the mixture from ethanol afforded *trans*-**2c** in pure form and a cis-rich mixture as a viscous oil. Data for *trans*-**2c**: 37% yield; light purple solids; mp 133−134 °C; MS *m*/*z* 548 (M^+); ^{1}H NMR (δ in $CDCl_3$) 0.33 (s, 18H, $SiMe_3$), 0.50 (s, 6H, *Me*SiPh), 7.15 (br.s, 2H, thiophene ring protons), 7.30−7.34 (m, 8H, Ph), 7.36−7.44 (m, 2H, Ph); ^{13}C NMR (δ in $CDCl_3$) −5.1 (*Me*SiPh), 0.0 ($SiMe_3$), 127.9 (*m*-Ph), 128.9 (*p*-Ph), 132.0 (*ipso*-Ph), 134.5 (*o*-Ph), 136.5 (C3 and C6), 139.4, 140.4 (C2, C7, C8a, and C8b), 152.0 (C3a and C5a); ^{29}Si NMR (δ in $CDCl_3$) −35.0 (SiMePh), −6.62 ($SiMe_3$). Anal. Calcd for $C_{28}H_{36}S_2Si_4$: C, 61.25; H, 6.60. Found: C, 61.29; H, 6.70. NMR data for *cis*-**2c** was obtained by subtracting the signals of *trans*-**2c** from the NMR spectra of the mixture: ^{1}H NMR (δ in $CDCl_3$) 0.49 (s, 6H, MeSiPh), signals due to Me_3Si and ring protons overlap with those of *trans*-**2c**; ^{13}C NMR (δ in $CDCl_3$) −5.0 (*Me*SiPh), 0.0 ($SiMe_3$,

(14) Yui, K.; Aso, Y.; Otsubo, T.; Ogura, F. *Bull. Soc. Chem.* **1989**, *62*, 1539.

overlapping with the signal of *trans*-**2c**), 127.6 (*m*-Ph), 128.8 (*p*-Ph), 132.4 (*ipso*-Ph), 134.6 (*o*-Ph), 135.4 (C3 and C6), 139.4 (overlapping with the signal of *trans*-**2c**), 140.6 (C2, C7, C8a, and C8b), 151.8 (C3a and C5a); ^{29}Si NMR (δ in $CDCl_3$) −34.4 (SiMePh), −6.62 ($SiMe_3$, overlapping with the signal of *trans*-**2c**).

Synthesis of Dibromodithienosilole 3a. To a 400 mL ether solution of 6.15 g (12.5 mmol) of compound **1a** was added dropwise 1.32 mL (25.6 mmol) of bromine at −90 °C, and the resulting mixture was stirred for 2 h at this temperature. After the solvent was removed under reduced pressure (15 mmHg), the residue was washed with hexane to give white solids, which were recrystallized from chloroform to give 4.17 g (66% yield) of **3a** as white solids: mp 262−266 °C; MS *m*/*z* 502 (M^+); ^{1}H NMR (δ in $CDCl_3$) 7.16 (s, 2H, thiophene ring protons), 7.34−7.47 (m, 6H, Ph), 7.58 (dd, 4H, J = 7.9, 1.3 Hz, *o*-Ph protons); ^{13}C NMR δ ($CDCl_3$) 112.4 (C2 and C6), 128.4, 130.3, 130.7 (Ph), 132.1 (C3 and C5), 135.5 (Ph), 139.3 (C7a and C7b), 150.0 (C3a and C4a). Anal. Calcd for $C_{20}H_{12}S_2SiBr_2$: C, 47.63; H, 2.40. Found: C, 47.51; H, 2.30.

Compound **3b** was prepared as described for **3a**. Data for **3b**: 65% yield; yellow solids; mp 200−202 °C; MS *m*/*z* 530 (M^+); ^{1}H NMR (δ in $CDCl_3$) 2.38 (s, 6H, *p*-Me), 7.21 (s, 2H, thiophene ring protons), 7.23 (d, 4H, J = 7.9 Hz, tolyl ring protons), 7.51 (d, 4H, J = 7.9 Hz, tolyl ring protons); ^{13}C NMR (δ in CD_2Cl_2) 21.7 (*p*-Me), 112.7 (C2 and C6), 127.1 (*p*-Tol), 129.5 (CH-Tol), 132.6 (C3 and C5), 135.6 (CH-Tol), 140.4 (Tol-*ipso*), 141.5 (C7a and C7b), 150.2 (C3a and C4a); ^{29}Si NMR (δ in $CDCl_3$) −18.7. Anal. Calcd for $C_{22}H_{16}Br_2S_2Si$: C, 49.63; H, 3.03. Found: C, 49.62; H, 3.01.

Synthesis of Dithienosilole 1e. To a solution of 2.0 g (4.0 mmol) of **3a** in 150 mL of ether was added 6.3 mL (8.0 mmol) of a 1.57 M *n*-butyllithium/hexane solution at −80 °C. After the resulting mixture was stirred at this temperature for 3.5 h, the mixture was hydrolyzed with saturated aqueous NH_4-Cl. After the usual workup, the resulting mixture was chromatographed on a silica gel column with hexane as eluent to give crude dark yellow solids, which were recrystallized from ether, affording 1.0 g (77% yield) of **1e** as pale yellow crystals: mp 140−143 °C; MS *m*/*z* 346 (M^+); ^{1}H NMR (δ in $CDCl_3$) 7.23 (d, 2H, J = 4.6 Hz, thiophene ring protons), 7.27 (d, 2H, J = 4.6 Hz, thiophene ring protons), 7.28−7.42 (m, 6H, Ph), 7.64 (dd, 4H, J = 7.9, 1.7 Hz, *o*-Ph protons); ^{13}C NMR (δ in $CDCl_3$) 125.9, 128.1, 129.6, 130.2, 131.8, 135.3 (Ph and thiophene carbons), 139.7 (C7a and C7b), 150.3 (C3a and C4a); ^{29}Si NMR (δ in $CDCl_3$) −20.7. Anal. Calcd for $C_{20}H_{14}S_2Si$: C, 69.32; H, 4.07. Found: C, 69.30; H, 4.06.

CV Measurements. CV measurements were carried out using a three-electrode system in an acetonitrile solution containing 100 mM of tetraethylammonium tetrafluoroborate as the supporting electrolyte and 4 mM of the substrate. Glassy carbon and Pt plate were used as the working and counter electrodes, and SCE was used as the reference electrode. The current−voltage curve was recorded at room temperature on a Hokuto Denko HAB-151 potentiostat/galvanostat.

X-ray Crystallographic Analysis of 2a,c. All unique diffraction maxima with $0 < 2\theta < 125.9°$ for **2a** and $0 < 2\theta < 126.1°$ for *trans*-**2c** were recorded on a Rigaku AFC-6C automated four-circle diffractometer using graphite-monochromated Cu Kα radiation (λ = 1.5418 Å). Refractions with $I > 3\sigma(I)$ were used in the least-squares refinement. The structure was solved by the SIR92 direct method[15] and expanded using DIRDIF94 Fourier techniques.[16] The non-hydrogen atoms were refined anisotropically. Neutral atom scattering factors were taken from Cromer and Waber.[17] Anomalous dispersion effects were included in F_c;[18] the values for $\Delta f'$ and $\Delta f''$ were those of Creagh and McAuley.[19] The values for the mass attenuation coefficients are those of Creagh and Hubbel.[20] All calculations were performed using the teXsan[21] crystallographic software package of Molecular Structure Corp.

Molecular Orbital Calculations on 1f, 2d, 4a, and 5. The ab initio MO calculations were carried out with the Gaussian 94 program at the RHF/6-31G level on a J932 server (Cray) at the Information Processing Center of Hiroshima University.

Preparation of EL Devices. Each layer of the EL devices was prepared by vacuum deposition at 1×10^{-5} Torr in the order of TPD, Alq3, and a silicon-bridged bithiophene (for a type I device only), on ITO coated on a glass substrate with a sheet resistance of 15 Ω/cm (Asahi Glass Co.). Finally, a layer of magnesium−silver alloy with an atomic ratio of 10:1 was vacuum-deposited as the top electrode. The thickness of each layer of the EL devices was measured with a Sloan Dektak 3030 surface profiler. The emitting area was 0.5×0.5 cm^2. Luminance was measured with a Topcon BM-7 luminance meter at room temperature.

Acknowledgment. The basic part of this work was supported by the Ministry of Education, Science, Sports and Culture (Grants-in-Aid for Scientific Research, No. 10133236 and 09450331). Application to EL devices was performed as a part of the Industrial Science and Technology Frontier Program by the New Energy and Industrial Technology Development Organization. We thank Sankyo Kasei Co. Ltd. and Sumitomo Electric Industry for financial support. We also thank Dr. Nakajima of Riken Keiki Co. Ltd. for the measurements of ionization potentials.

Supporting Information Available: Tables of atomic coordinates, anisotropic thermal parameters, and bond distances and angles for **2a** and *trans*-**2c**. This material is available free of charge via the Internet at http://pubs.acs.org.

OM980918N

(15) Altomare, A.; Burla, M. C.; Camalli, M.; Cascarano, M.; Giacovazzo, C.; Guagliardi, A.; Polidori, G. *J. Appl. Crystallogr.* **1994**.
(16) Beurskens, P. T.; Admiraal, G.; Beurskens, G.; Bosman, W. P.; de Gelder, R.; Israel, R.; Smits, J. M. M. The DIRDIF-94 program system; Technical Report of the Crystallography Laboratory; University of Nijmegen, Nijmegen, The Netherlands, 1994.
(17) Cromer, D. T.; Waber, J. T. In *International Tables for X-ray Crystallography*; Kynoch Press: Birmingham, England, 1974; Vol. IV, Table 2.2A, 1974.
(18) Ibers, J. A.; Hamilton, W. C. *Acta Crystallogr.* **1964**, *17*, 781.
(19) Creagh, D. C.; McAuley, W. J. In *International Tables for Crystallography*; Wilson, A. J. C., Ed.; Kluwer Academic: Boston, 1992; Vol. C, Table 4.2.6.8, pp 219−222.
(20) Creagh, D. C.; Hubbell, J. H. In *International Tables for Crystallography*; Wilson, A. J. C., Ed.; Kluwer Academic: Boston, 1992; Vol. C, Table 4.2.4.3, pp 200−206.
(21) teXsan: Crystal Structure Analysis Package; Molecular Structure Corp., The Woodlands, TX, 1985 & 1992.